Density functional theory study of the oxoperoxo vanadium(V) complexes of glycolic acid. Structural correlations with NMR chemical shifts

Licínia L. G. Justino,*[a,d] M. Luísa Ramos,[a,d] Martin Kaupp,[b] Hugh D. Burrows,[a] Carlos Fiolhais[c] and Victor M. S. Gil[a]

Received 26th May 2009, Accepted 19th August 2009
First published as an Advance Article on the web 7th September 2009
DOI: 10.1039/b910033d

The DFT B3LYP/SBKJC method has been used to calculate the gas-phase optimized geometries of the glycolate oxoperoxo vanadium(V) complexes $[V_2O_2(OO)_2(gly)_2]^{2-}$, $[V_2O_3(OO)(gly)_2]^{2-}$ and $[VO(OO)(gly)(H_2O)]^-$. The ^{51}V, ^{17}O, ^{13}C and ^{1}H chemical shifts have been calculated for the theoretical geometries in all-electron DFT calculations at the UDFT-IGLO-PW91 level and have been subsequently compared with the experimental chemical shifts in solution. In spite of being applied to the isolated molecules, the calculations allowed satisfactory reproduction of the multinuclear NMR solution chemical shifts of the complexes, suggesting that the theoretical structures are probably close to those in solution. The effects of structural changes on the ^{51}V and ^{17}O NMR chemical shifts have been analysed using the referred computational methodologies for one of the glycolate complexes and for several small molecules taken as models. These calculations showed that structural modifications far from the metal nucleus do not significantly affect the metal chemical shift. This finding explains why it is possible to establish reference scales that correlate the type of complex (type of metal centre associated with a certain type of ligand) with its typical region of metal chemical shifts. It has also been found that the V=O bond length is the dominant geometrical parameter determining both $\delta^{51}V$ and the oxo $\delta^{17}O$ in this kind of complex.

Introduction

Since the 1970s it has been known that vanadium plays an essential role in a number of biochemical processes, including the synthesis of chlorophyll and the normal growth of some animals.[1] Over the last few decades, *in vivo* and *in vitro* studies of the biological effects[2] of this metal have revealed other important properties, such as the ability to inhibit some enzymes, in addition to antitumorigenic[3,4] and insulinomimetic effects.[5,6]

Vanadium oxoperoxocomplexes are an important class of vanadium compounds, due to their biological and industrial applications. These complexes show antitumorigenic[4] activity and also enhanced insulinomimetic[6,7] activity compared with the anionic salts of vanadium. Additionally, they have been studied as functional models[8-10] for the haloperoxidase enzymes and are efficient oxidants for several substrates, including benzene and other aromatics, alkenes, allylic alcohols, sulfides, halides, and primary and secondary alcohols.[11-13]

α-Hydroxycarboxylic acids are important biogenic ligands, since they are involved in many basic biochemical processes, such as the Krebs cycle (malate, citrate, isocitrate), Cori cycle (lactate), photorespiration (glycolate), *etc*. The complexes which result from the association of vanadium, peroxide and these acids are, thus, potentially biochemically relevant molecules. Following this interest, we have carried out studies on V(V)–acid–H_2O_2 systems.[14-17] Previously,[15] some of us have studied the system V(V)–glycolic acid–H_2O_2 in aqueous solution using NMR spectroscopy and have proposed structures for the oxoperoxo vanadium(V) complexes of this acid present in solution. The solid state structure of one of these complexes is known,[18] but no detailed information has been reported on the structure of the remaining complexes found in aqueous solution. In this paper we apply DFT to further characterize the structures of these species and to understand the major structural features determining their metal and oxo oxygen chemical shifts in their NMR spectra. For this, we will carry out DFT calculations of the structures and of their NMR chemical shifts, and we will study how these vary with structural modification. We will also consider small vanadium molecules as model compounds for the calculation of structural effects.

Results and discussion

Theoretical structures

In our NMR study of the ternary system V(V)–glycolic acid–H_2O_2 in aqueous solution,[15] we detected six complexes, three of which are present in very small amounts. We have proposed structures for the three major complexes, one symmetrical 2:2:2 (metal:acid:peroxide) complex (**G-2**), one asymmetrical 2:2:1 complex (**G-1**) and one 1:1:1 complex (**G-3**). Their structures have seven-coordinated oxoperoxo vanadium centres (**G-1**, **G-**

[a]*Departamento de Química, Faculdade de Ciências e Tecnologia, Universidade de Coimbra, 3004-535, Coimbra, Portugal. E-mail: liciniaj@qui.uc.pt*
[b]*Institut für Anorganische Chemie, Universität Würzburg, Am Hubland, D-97074, Würzburg, Germany*
[c]*Departamento de Física e Centro de Física Computacional, Faculdade de Ciências e Tecnologia, Universidade de Coimbra, 3004-516, Coimbra, Portugal*
[d]*Centro de Neurociências e Biologia Celular, Faculdade de Ciências e Tecnologia da Universidade de Coimbra, 3004-517, Coimbra, Portugal*

2 and **G-3**) and a five coordinated dioxo vanadium centre (**G-1**). In the present study we have considered these structures and, additionally, we have tested a second possible structure for **G-2** (which is equally in agreement with the experimental NMR results[15]). We have chosen the DFT B3LYP/SBKJC calculation level to optimize the structures since this method has proved to be reasonable for the study of oxoperoxo vanadium(V) complexes of α-hydroxycarboxylic acids.[17]

In Fig. 1, we present the optimized geometries of the structures under study. **G-2*syn*** and **G-2*anti*** are the two structures under analysis for **G-2** and are isomers differing in the relative orientation of the V=O bonds. Interestingly, for achiral ligands only structures having an *anti* orientation of the V=O bonds have been found in the solid state. For chiral ligands, both *syn* and *anti* orientations are found, depending on the combination of two L,L (or D,D) or L,D ligands.[19] These differences are not yet understood. We present here a possible explanation: while for a L-ligand (or a D-ligand) a symmetrical structure is obtained only if the V=O bonds adopt a *syn* orientation, for L,D-ligands the symmetry can be achieved by having the two V=O bonds *anti* to each other. This natural willingness for structural symmetry is merely the consequence of repetition of the most stable arrangement of a fraction of the molecule. For an achiral ligand, such as glycolic acid, both *syn* and *anti* arrangements lead to symmetrical structures. In this case, the mutual arrangement of the V=O bonds is constrained only by the repulsions between the oxo and the peroxo ligands. Apparently, **G-2*anti*** should be more stable since it presents the arrangement that minimizes the V=O repulsions. In our study we will analyze if it is possible to obtain any indication from the calculations of increased stability of one form or the other.

As a starting point for **G-1**, we have taken a structure having one dioxo vanadium centre (V1), with a coordination number of five, and one oxoperoxo seven-coordinated vanadium centre (V2), with a bonded water molecule (this structure is slightly different from the one we proposed earlier,[15] which involved an oxo vanadium centre with a water molecule bridging the two vanadium atoms). In the optimization of **G-1** the water molecule initially bonded to V2 is expelled from the metal coordination sphere, and remains only as a species hydrogen-bonded to the peroxo oxygens and to O4, leading to the geometry **G-1.**H_2O (Fig. 1). The coordination number of this centre is, thus, reduced from seven to six. This result has been found previously in our study of the L-lactate oxoperoxo vanadium(V) complexes[17] and by Bühl *et al.*[20] in the DFT optimization of $[VO(O_2)_2(H_2O)_2]^-$, which converged to produce $[VO(O_2)_2(H_2O)]^-$. Removal of this water molecule and reoptimization afforded **G-1**. We have also considered structures having seven-coordinated oxoperoxo centres with a bonded water molecule as starting structures for **G-2*anti***, **G-2*syn*** and **G-3**. Also in these cases, one water molecule is expelled in their optimization and remains hydrogen-bonded to the complex. In **G-3** the water molecule *trans* to V=O is expelled, presumably due to a weakening of the *trans* bond caused by the O^{2-} (oxo) ligand, that is, a *trans* effect. All the structures have been reoptimized after removal of these water molecules, leading to the geometries presented in Fig. 1. It is significant that, by losing its two coordinated water molecules during the optimization, **G-2*anti*** converged to

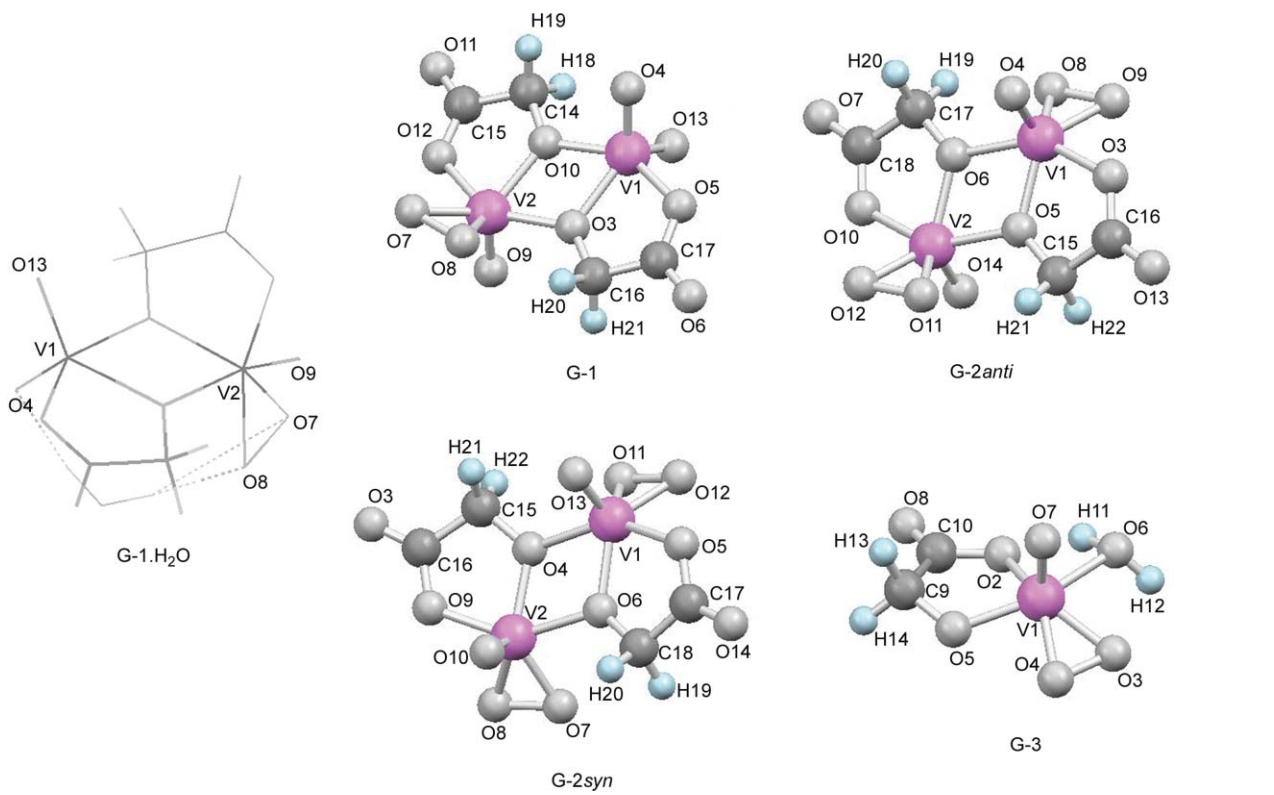

Fig. 1 Optimized geometries **G-1.**H_2O, **G-1** (results from optimization of **G-1.**H_2O after removal of the hydrogen bonded H_2O molecule), **G-2*anti***, **G-2*syn*** and **G-3** (calculated at the B3LYP/SBKJC level).

a structure similar to the only known solid state structure[18] for this system.

To try to assess which of the isomers **G-2*syn*** or **G-2*anti*** is more stable, we have calculated the energies (with the zero point corrections) of their equilibrium geometries. The results indicate **G-2*syn*** as being 0.1 kcal mol^{-1} more stable than **G-2*anti***. This energy difference is, however, too small to be considered as significant and, thus, does not allow any conclusion.

As a test of the quality of the predicted structures, we have calculated their isotropic ^{51}V, ^{17}O, ^{13}C and ^{1}H chemical shifts using the UDFT-IGLO-PW91 method, which we have previously tested in the study of a related system.[17] We compare in Table 1 the theoretical chemical shifts with the experimental solution shifts available from our previous NMR study.[15] The comparison of the gas phase SBKJC/B3LYP calculated structure of **G-2*anti*** with its solid state structure has not been attempted because the reported data[18] for the crystal is not clear.

When comparing the computed and the experimental chemical shifts of Table 1 we have to take into account the fact that the experimental chemical shifts were obtained for the molecules in solution at approximately 293 K, whereas the theoretical chemical shifts were calculated for the isolated molecules in their (static) gas phase equilibrium geometries. This means that we are neglecting solvent, rovibrational and zero-point effects on the chemical shifts (more correctly, these effects are not entirely neglected, but rather assumed to be similar in the molecules under study and the reference compounds), and we are also neglecting solvent effects in the optimization procedure (gas phase optimization; see Computational Details). The differences between theoretical and experimental chemical shifts are, thus, partly due to approximations assumed in the chemical shift calculation, partly due to intrinsic differences between the solution and gas phase structures and partly due to errors of the calculation methods themselves (these refer mainly to deficiencies of the exchange–correlation functionals and to basis set limitations). To evaluate approximately the effect on the metal chemical shift of neglecting the solvent we have calculated the $\delta(^{51}\mathrm{V})$ of **G-3** having six water molecules hydrogen bonded to it. The difference between the experimental and calculated chemical shifts is reduced to 131.2 ppm, meaning an improvement of 21.4 ppm (*cf*. Table 1). The importance of solvent effects on ^{51}V shifts has also been studied for the anion $H_2VO_4^-$, for which the addition of two water molecules leads to an improvement of 64 ppm in the calculated $\delta(^{51}\mathrm{V})$.[21] In addition to these direct effects, indirect effects may also be expected, since the intermolecular interactions established between solvent molecules and the complex will also modify the structures, consequently affecting their chemical shifts.

Comparing the results for **G-2*anti*** with those for **G-2*syn***, we see that the first structure allows a slightly better reproduction of the experimental chemical shifts of the **G-2** complex in solution. Although we cannot exclude the **G-2*syn*** structure, there is no indication from our calculations that this structure should be preferred over **G-2*anti***. Therefore, we feel that the *anti* arrangement of the V=O bonds found in the solid state[18] is, probably, maintained in solution.

Focusing on the chemical shifts of **G-1**, **G-2*anti*** and **G-3**, we notice that the theoretical ^{51}V shift of the dioxo vanadium centre has a difference relative to the experimental value of *ca.* 30 ppm, while those of the oxoperoxo vanadium centres show differences from 144.3 to 157.9 ppm. These differences are in agreement with those obtained previously in our study of the lactate oxoperoxo V(V) complexes and indicate some difficulties with the geometrical description of the oxoperoxo centres.[17] In

Table 1 Computed and experimental isotropic chemical shifts for the complexes of Fig. 1[a]

Molecule	Site	δiso$_{calc}$[b]	δiso$_{expt}$[c]	Difference (ppm)
G-1				
	V(1)	–483.7	–514.2	30.5
	V(2)	–436.1	–580.4	144.3
	O(4)	1029.7	—	—
	O(7)	721.5	—	—
	O(8)	708.5	—	—
	O(9)	1035.2	—	—
	O(13)	1025.9	—	—
	C(14)	84.53	78.50	6.03
	C(15)	181.58	183.89[d]	–2.31
	C(16)	80.98	75.06	5.92
	C(17)	182.74	184.99[d]	–2.25
	H(18)	3.85	4.87/4.58[e]	–1.02/–0.73
	H(19)	3.83	4.58/4.87	–0.75/–1.04
	H(20)	5.18	5.32/5.25	–0.14/–0.07
	H(21)	4.43	5.25/5.32	–0.82/–0.89
G-2*syn*				
	V(1);V(2)	–415.2; –414.3	-582.8	167.6;168.5
	O(7);O(11)	715.4; 720.5	—	—
	O(8);O(12)	727.4;718.0	—	—
	O(10);O(13)	1040.7;1041.5	1184.2	–143.5; –142.7
	C(15);C(18)	85.80;85.07	74.56	11.24; 10.51
	C(16);C(17)	182.53;182.15	185.80	–3.27; –3.65
	H(19);H(22)	4.92;4.81	5.32/5.23	–0.40/–0.31; –0.42/–0.51
	H(20);H(21)	4.44;4.59	5.23/5.32	–0.79/–0.88; –0.73/–0.64
G-2*anti*				
	V(1);V(2)	–424.9	–582.8	157.9
	O(4);O(14)	1041.5	1184.2	–142.7
	O(8);O(11)	708.2	—	—
	O(9);O(12)	726.0	—	—
	C(15);C(17)	82.69	74.56	8.13
	C(16);C(18)	182.26	185.80	–3.54
	H(19);H(21)	5.24	5.32/5.23	–0.08/0.01
	H(20);H(22)	4.27	5.23/5.32	–0.96/–1.05
G-3				
	V(1)	–421.4	–574.0	152.6
	O(3)	666.6	—	—
	O(4)	756.4	—	—
	O(7)	1016	—	—
	C(9)	84.51	75.16	9.35
	C(10)	185.81	185.69	0.12
	H(13)	4.93	5.41/5.01	–0.48/–0.08
	H(14)	4.36	5.01/5.41	–0.65/–1.05

[a] UDFT-IGLO-PW91 calculations at B3LYP/SBKJC optimized structures. [b] ^{51}V, ^{13}C and ^{1}H isotropic chemical shifts are given with respect to the calculated shielding values of $VOCl_3$ and TMS (σ(V) = –1945.7 ppm, σ(C) = 182.96 ppm, σ(H) = 30.54 ppm). [c] From ref. 15. [d] There is the possibility of a reverse assignment between C(15) and C(17). [e] The oblique line indicates the possibility of a reverse attribution.

Table 2 Computed and experimental ^{51}V chemical shifts and $\Delta\delta$ values[a]

	δ_{exp}[b]	$\Delta\delta_{exp}$[c]	δ_{calc}[d]	$\Delta\delta_{calc}$[c]
G-1 $[V_2O_3(OO)(gly)_2]^{2-}$	(−514.2)[e]; −580.4	−44.1	(−483.7); −436.1	−23.5
G-2*anti* $[V_2O_2(OO)_2(gly)_2]^{2-}$	−582.8	−46.5	−424.9	−12.3
G-3 $[VO(OO)(gly)(H_2O)]^-$	−574.0	−37.7	−421.4	−8.8

[a] Computational results at UDFT-IGLO-PW91//B3LYP/SBKJC level, relative to $VOCl_3$ ($\sigma(^{51}V) = -1945.7$ ppm). [b] *Cf*. ref 15. [c] $\Delta\delta = \delta$complex − $\delta[VO(OO)(H_2O)_3]^+$; applied only to the oxoperoxo V(V) centres. $\delta_{expt}[VO(OO)(H_2O)_3]^+ = -536.3$ ppm; $\delta_{cal}[VO(OO)(H_2O)_3]^+ = -412.6$ ppm. [d] Calculated isotropic chemical shifts (ppm) relative to $VOCl_3$ ($\sigma(^{51}V) = -1945.7$ ppm). [e] Values in parentheses refer to the V(V) dioxo centre.

contrast, the chemical shift prediction for the dioxo centre is excellent (an error of 0.9% of the total vanadium chemical shift range, 3500 ppm), indicating this provides a very good description of the geometry of this centre. The differences for the oxoperoxo centres are within the usual results: For example, Bühl and Hamprecht[22] obtained, for a set of vanadium(V) oxocomplexes, a mean absolute difference between calculated and experimental ^{51}V chemical shifts of 169 ppm, 114 ppm, 119 ppm and 118 ppm, respectively, at the PW91/SOS-DFPT-LOC1/IGLO, BP86/GIAO, B3LYP/GIAO and B3LYP/IGLO levels. For the diperoxocomplex $[VO(O_2)_2(H_2O)_2]^-$, Bühl and Parrinello,[20] at the B3LYP/GIAO level, obtained differences between the experimental (−692 ppm) and the predicted ^{51}V shifts from 37 to 128 ppm (several structures were considered resulting from optimization at different levels).

Table 2 shows the experimental and theoretical $\Delta\delta$ values obtained for the ^{51}V shifts of the complexes under study. These $\Delta\delta$ values are the shifts upon complexation calculated relative to the monoperoxo vanadate $[VO(OO)(H_2O)_3]^+$. For all the cases we were able to correctly predict that the magnetic shielding of the metal is larger in the complex relative to its value in $[VO(OO)(H_2O)_3]^+$ (that is, $\Delta\delta < 0$). Additionally, we correctly predict that the metal is more shielded in **G-1** and **G-2*anti*** than it is in **G-3**. We see that, in spite of some difficulties in predicting absolute ^{51}V shifts for the oxoperoxo centres, it is possible to correctly predict relative differences of ^{51}V shifts between complexes. Similar conclusions were obtained for the L-lactic acid oxoperoxo vanadium(V) complexes.[17]

Considering the $^{17}O(V{=}O)$ chemical shifts, the only complex for which the experimental shift is known is **G-2*anti***, with a difference between the calculated and experimental values of −142.7 ppm (Table 1). This difference also provides an indication of some difficulties in calculating the geometry of the oxoperoxo centres. We have previously attributed this to overestimation of the O–O bond lengths.[17] In spite of these problems, the calculations correctly predict that the magnetic shielding of the V=O oxygen nucleus of the oxoperoxo center is larger in **G-2*anti*** than in $[VO(OO)(H_2O)_3]^+$ ($\Delta\delta_{expt} = -56$ ppm and $\Delta\delta_{calc} = -133$ ppm; $\delta_{expt}[VO(OO)(H_2O)_3]^+ = 1240$ ppm and $\delta_{calc}[VO(OO)(H_2O)_3]^+ = 1174$ ppm). We have not found any other calculation in the literature of ^{17}O shifts for oxoperoxo vanadium(V) complexes (besides our previous work[17]). The shifts of the peroxo oxygen atoms have not been observed experimentally due to their broadening arising from fast relaxation. The computed shifts presented in Table 1 for these atoms are, thus, predictions. The values obtained are consistent with the experimental ^{17}O O–O shifts of $[VO(OO)]^+$ (660 ppm) and of $VO(OO)(pic)(H_2O)_2$ (641 ppm).[23]

For the ^{13}C and ^{1}H chemical shifts, we obtained absolute differences between theoretical and experimental shifts ranging from 0.12 to 9.35 ppm and 0.01 to 1.05 ppm, respectively. For the ^{13}C chemical shifts of the three complexes, the mean absolute deviation from experiment is 4.93 ppm, which corresponds to 2.47% of the ^{13}C total chemical shift range (*ca.* 200 ppm), which seems a relatively good result. Additionally, the correlation of $\delta(^{13}C)_{exp}$ *vs.* $\delta(^{13}C)_{calc}$ has the reasonable slope of 1.1. The quality of the ^{1}H predicted shifts is somewhat inferior. This is expected at this level of calculation since the ^{1}H shifts are extremely sensitive to the neglect of solvation and H-bonding effects.

Finally, we present in Table 3 some geometrical parameters of the gas phase structures of the complexes **G-1**, **G-2*anti*** and **G-3**.

Structural effects on ^{51}V and ^{17}O chemical shifts

In this section we will try to clarify how some structural features of oxoperoxo complexes of V(V) influence their ^{51}V and ^{17}O NMR chemical shifts. We will start by considering the coordination of a small ligand, then the substitution of a fragment of a ligand and finally the modification of some geometrical parameters.

Coordination of a small ligand

Previously[14,15] we have proposed that $[VO(OO)(gly)(H_2O)_2]^-$, with a coordination number of seven, and $[VO(OO)(L\text{-lact})(H_2O)]^-$, with a coordination number of six, give rise to the ^{51}V signals at $\delta_V = -574.0$ ppm and $\delta_V = -546.0$ ppm, respectively and $[VO(OO)(L\text{-malat})(H_2O)]^-$ and $[VO(OO)(L\text{-malat})(H_2O)_2]^-$ produce signals at $\delta_V = -537.4$ and $\delta_V = -575.4$ ppm, respectively.[16] These attributions were based on our hypothesis that the coordination of an electron donating ligand, such as water, would increase the metal magnetic shielding. This hypothesis follows from the experimental observation that the substitution of a weak electron donor (H_2O) by a stronger one increases the shielding of the metal (*e.g.*, $\delta^{51}V$ is −536.3 ppm for $[VO(OO)(H_2O)_3]^+$ and around −595 ppm for the oxomonoperoxo complexes of α-hydroxycarboxylic acids). To confirm the validity of this, we have calculated the metal chemical shifts for the above complexes of glycolic and L-lactic acids and also for $[VO(OO)(gly)(H_2O)]^-$ and $[VO(OO)(L\text{-lact})(H_2O)_2]^-$ (Fig. 2 and Table 4).

From Table 4, we can conclude that the effect of the coordination of the water ligand is, in fact, that of increasing the shielding of the metal. The observed effect, a more negative shift of *ca.* 50 ppm, is in excellent accord with the experimental difference between the two complexes of L-malate (−38 ppm). Considering $[VO(OO)(L\text{-lact})(H_2O)]^-$ and $[VO(OO)(gly)(H_2O)_2]^-$, the calculation predicts a difference of −57.7 ppm (*i.e.* a more negative shielding for the second complex), whilst the experimental difference is −28.0 ppm. While for the peroxide species analyzed in this work and in ref. 24 only the effect described above has been found, an opposite

Table 3 Selected B3LYP/SBKJC optimized structural parameters (bond lengths in Å, bond angles in deg) for glycolic acid V(V) complexes

G-1		**G-2*anti***		**G-3**	
V1–O4	1.6425	V1–O8	1.8789	V1–O6	2.2144
V1–O13	1.6415	V1–O9	1.8746	V1–O7	1.6125
V1–O3	2.0320	V1–O3	2.0472	V1–O2	2.0491
V1–O5	1.9938	V1–O5	1.9677	V1–O5	1.9122
V1–O10	2.0103	V1–O6	2.0707	V1–O3	1.8723
V2–O7	1.8765	V1–O4	1.6139	V1–O4	1.9032
V2–O8	1.8820	V2–O11	1.8789	O3–O4	1.5029
V2–O9	1.6128	V2–O12	1.8746	C9–O5	1.4389
V2–O3	2.0403	V2–O6	1.9677	C9–C10	1.5535
V2–O10	1.9974	V2–O14	1.6139	O2–C10	1.3586
V2–O12	2.0506	V2–O5	2.0706	O5–C10	1.2617
O7–O8	1.5027	V2–O10	2.0472	O7–V1–O4	108.41
O4–V1–O13	109.69	O8–O9	1.5022	O6–V1–O2	66.87
O10–V1–O13	98.89	O11–O12	1.5022	O7–V1–O2	105.31
O5–V1–O4	100.81	O4–V1–O8	108.23	O6–V1–O7	94.12
O7–V2–O9	109.44	O4–V1–O9	110.45	O2–V1–O5	77.56
O8–V2–O9	107.91	O4–V1–O6	94.16	O2–V1–O4	143.84
O7–V2–O8	47.13	O11–V2–O14	108.23	O2–V1–O3	127.45
O9–V2–O12	95.43	O12–V2–O14	110.46	O6–V1–O5	142.96
O3–V2–O9	95.96	O5–V2–O14	94.16	O7–V1–O3	112.90

Table 4 ^{51}V calculated chemical shifts for **G-3**, **G-3**·H_2O, **L-3*cis*** and **L-3*cis***·H_2O (computed using the UDFT-IGLO-PW91 approximation)

Complex	δ^{51}V/ppm	
$[VO(OO)(gly)(H_2O)]^-$	−421.4	
$[VO(OO)(gly)(H_2O)_2]^-$	−466.4	$\Delta\delta_{\text{G-3}\rightarrow\text{G-3H2O}} = -45.0$ ppm
$[VO(OO)(L\text{-lact})(H_2O)]^-$	−408.7	
$[VO(OO)(L\text{-lact})(H_2O)_2]^-$	−461.8	$\Delta\delta_{\text{L-3}cis\rightarrow\text{L-3}cis\text{H2O}} = -53.1$ ppm

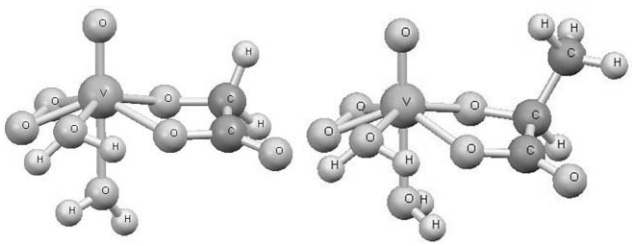

Fig. 2 **G-3.**H_2O and **L-3*cis*.**H_2O; the structures were constructed by addition of one water molecule in an apical position to **G-3** and **L-3*cis***,[17] respectively, assuming the value calculated for the equatorial water molecule for the V–OH_2 bond length.

effect has been reported for non peroxidic species in the series VOX_3 (X = F, Cl, Br), with a decrease of the metal shielding as the electron donating properties of the ligands increase.[25]

Substitution of a fragment of the ligand

We have replaced one of the hydrogen atoms of CH_2O^- of **G-3** (Fig. 1) by the fragment CH_3, without any further changes (Fig. 3). We have calculated the ^{51}V magnetic shielding constant for this arrangement and in Table 5 we compare the localized molecular orbital (LMO) contributions to the shielding in **G-3** with the contributions in this new structure, **G-3′**, a "pseudo" lactic acid complex. The aim of this experiment is to understand why the ^{51}V chemical shifts of homologous oxomonoperoxo complexes of V(V) with different α-hydroxycarboxylic acids fall within a small range of values (see, for example, refs 14–16 and 48).

Table 5 Localized molecular orbital contributions to the ^{51}V magnetic shielding in **G-3** and in **G-3′**

LMO	**G-3**	**G-3′**	Δ_{cont} [a]
Σ(AO V(1))	1696.2	1699.8	3.6
Lone Pair V(1)	−10.2	0.1	10.3
Σ(AO O(7))	−31.8	−30.9	0.9
Σ(Bond V(1)–O(7))	−1104.9	−1108.1	−3.2
Lone Pair O(5)	−7.9	−4.9	3.0
Σ(Lone Pair O(6))	−82.9	−83.0	−0.1
Lone Pair O(3)	−7.4	−6.9	0.5
Lone Pair O(8))	−0.3	−0.3	0
Bond O(2)–H(11)	−3.3	−2.9	0.4
Lone Pair O(4)	−19.4	−19.5	−0.1
Bond C(9)–C(10)	−17.3	−16.3	1.0
Bond O(6)–H(11)	−3.7	−3.6	0.1
Bond H(13)–C(9)[b]	−5.5	—	—
Bond O(2)-C(10)	−14.4	−14.7	−0.3
Bond H(14)–C(9)	−14.2	−13.5	0.7
Bond O(8)–C(10)	−6.6	−6.7	−0.1
Bond H(12)–O(6)	−3.3	−3.3	0
Bond O(5)–C(9)	−13.9	−11.4	2.5
AO O(2)	−6.6	−6.3	0.3
Bond O(3)–O(4)	−4.5	−4.4	0.1
AO O(4)	−61.5	−60.0	1.5
AO O(3)	−68.4	−69.5	−1.1
Lone Pair O(2)	−-221.0	−219.8	1.2
Bond O(8)–C(10)	−1.5	−2.0	−0.5
AO O(5)	−66.8	−63.8	3.0
Bond O(5)–V(1)	−404.3	−412.7	−8.4
Bond O(4)–V(1)	−498.1	−496.9	1.2
AO O(8)	−8.5	−8.7	−0.2
Bond O(3)–V(1)	−541.6	−542.6	−1.0
Bond H(17)—C(13)	—	−2.4	—
Bond H(16)–C(13)	—	−2.7	—
Bond C(13)–C(9)	—	−1.8	—
Bond H(15)–C(13)	—	−0.2	—
$\Sigma_{cont} = \sigma(^{51}V)$	−1524.3	−1520.0	$\Sigma\Delta_{cont} = 4.3$

[a] Δ_{cont} = contribution in **G-3′** – contribution in **G-3**. [b] H(13)–C(1) refers to a bond of **G-3**. H(13) of **G-3** was replaced by CH_3 to give **G-3′**.

The replacement of the H atom by a CH_3 group causes a change of 4.3 ppm in the metal magnetic shielding ($\Sigma\Delta_{cont}$). We see, thus, that structural modifications far from the metal nucleus

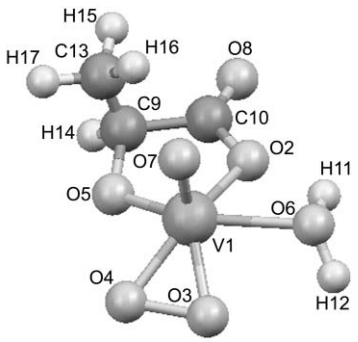

Fig. 3 Structure of **G-3′** (**G-3** having the hydrogen atom H(13) of CH_2O^- replaced by CH_3).

do not significantly affect the metal chemical shift, even when these changes involve the replacement of a ligand (by replacing one H atom of glycolic acid we obtain lactic acid). This result explains why we can establish reference scales that correlate the type of complex (type of metal centre associated with a certain type of ligand) with its typical range of ^{51}V chemical shifts, such as that formulated by Rehder[26] for V(V) complexes with biogenic ligands.

Modification of bond lengths

Table 6 shows the LMO contributions for **G-3″** and for **G-3‴**, in which the V–OCO and V=O bond lengths have been increased by 0.1 Å relative to their values in **G-3**. In these two cases the effects are more pronounced, in comparison with the previous situation. For the increase of the V–OCO bond length the change of the metal magnetic shielding is –38.8 ppm and for the increase of the V=O bond length the change is –243.0 ppm. Looking at the individual contributions, we see that, as expected, the greater differences come from the contributions of the orbitals localized on the regions that have been modified, that is, for **G-3″**, the contributions from the lone pair in O(2) (and also from the O(5)–V(1) bond), and for **G-3‴**, the contribution from the V(1)–O(7) bond.

Studies on model molecules

To evaluate the dependence of the ^{51}V and ^{17}O chemical shifts on geometrical parameters, we have calculated the shielding constants for these nuclei on three systems, taken as models, in which we varied several structural parameters. We have considered, specifically, $[VO_2]^+$, $[VO(OO)]^+$ and $[VO_2(gly)(H_2O)]^-$. The first two are models for the metal centres found in oxoperoxo vanadium(V) complexes, while the last, besides being a model for dioxo vanadium(V) complexes, constitutes a test for the possibility of transposing the results obtained for $[VO_2]^+$ and $[VO(OO)]^+$ to other complexes. In the initial analysis, these results allow the evaluation of the contribution of structure deficiencies to the errors in the calculated chemical shifts. Additionally, in cases where the effects of the substituents are not substantial, they may permit the

Table 6 Localized molecular orbital contributions to the ^{51}V magnetic shielding in **G-3**, **G-3″** and **G-3‴**

LMO	G-3	G-3″[a]	$\Delta_{cont\ G\text{-}3''}$[b]	G-3‴[c]	$\Delta_{cont\ G\text{-}3'''}$
Σ(AO V(1))	1696.2	1697.5	1.3	1703.8	7.6
Lone Pair V(1)	–10.2	–14.5	–4.3	—	—
Σ(AO O(7))	–31.8	–32.9	–1.1	–26.3	5.5
Σ(Bond V(1)–O(7))	–1104.9	–1098.0	6.9	–1238.0	–133.1
AO O(5)	–66.8	–75.2	–8.4	–81.0	–14.2
Bond O(5)–V(1)	–404.3	–420.9	–16.6	–421.2	–16.9
Bond O(5)–C(9)	–13.9	–15.1	–1.2	–13.8	0.1
Lone Pair O(5)	–7.9	–7.6	0.3	–8.5	–0.6
AO O(4)	–61.5	–64.3	–2.8	–75.0	–13.5
Bond O(4)-V(1)	–498.1	–506.3	–8.2	–514.7	–16.6
Lone Pair O(4)	–19.4	–20.5	–1.1	–19.7	–0.3
AO O(3)	–68.4	–69.4	–1.0	–79.1	–10.7
Bond O(3)–V(1)	–541.6	–545.1	–3.5	–555.1	–13.5
Lone Pair O(3)	–7.4	–7.9	–0.5	–7.9	–0.5
Bond O(3)–O(4)	–4.5	–4.4	0.1	–3.5	1.0
AO O(2)	–6.6	—	—	–8.7	–2.1
Bond V(1)-O(2)	—	—	—	–17.9	—
Bond O(2)–H(11)	–3.3	–2.7	0.6	–3.5	–0.2
Lone Pair O(2)	–221.0	–205.8	15.2	–228.5	–7.5
Bond O(2)–C(10)	–14.4	–15.6	–1.2	–15.0	–0.6
Σ(Lone Pair O(6))	–82.9	–87.8	–4.9	–86.0	–3.1
Lone Pair O(8))	–0.3	–0.5	–0.2	–0.4	–0.1
AO O(8)	–8.5	–11.0	–2.5	–10.1	–1.6
Bond C(9)–C(10)	–17.3	–18.3	–1.0	–18.9	–1.6
Bond O(6)-H(11)	–3.7	–3.0	0.7	–4.0	–0.3
Bond H(13)–C(9)	–5.5	–6.2	–0.7	–6.9	–1.4
Bond H(14)–C(9)	–14.2	–14.6	–0.4	–15.3	–1.1
Σ(Bond O(8)–C(10))	–8.1	–9.7	–1.6	–8.8	–0.7
Bond H(12)–O(6)	–3.3	–3.4	–0.1	–3.5	–0.2
$\Sigma_{cont} = \sigma(^{51}V)$	–1524.3	–1563.1	$\Sigma\Delta_{cont} = -38.8$	–1767.3	$\Sigma\Delta_{cont} = -243.0$

[a] In **G-3** r(V–OCO) = 2.049106 Å; in **G-3″** r(V–OCO) = 2.149106 Å (+4.9%). [b] Δ_{cont} = contribution in the structure–contribution in **G-3**. [c] In **G-3** r(V=O) = 1.6125 Å; in **G-3‴** r(V=O) = 1.7125 Å (+6.2%).

prediction of changes in the ^{51}V and ^{17}O chemical shifts between complexes based on their structural differences.

(a) Molecular model $[VO_2]^+$

The DFT optimized geometry of $[VO_2]^+$ is presented on Fig. 4. Starting from this geometry, we have modified the V=O bond lengths and the O=V=O angle. For the various structures obtained in this manner, we have calculated the magnetic shielding constants for the metal and for the oxygen atoms, which were plotted as a function of the corresponding structural parameter (Fig. 5 shows the plots for the modification of the V=O bonds).

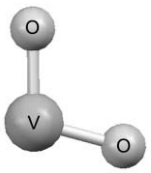

Fig. 4 SBKJC/B3LYP structure of $[VO_2]^+$.

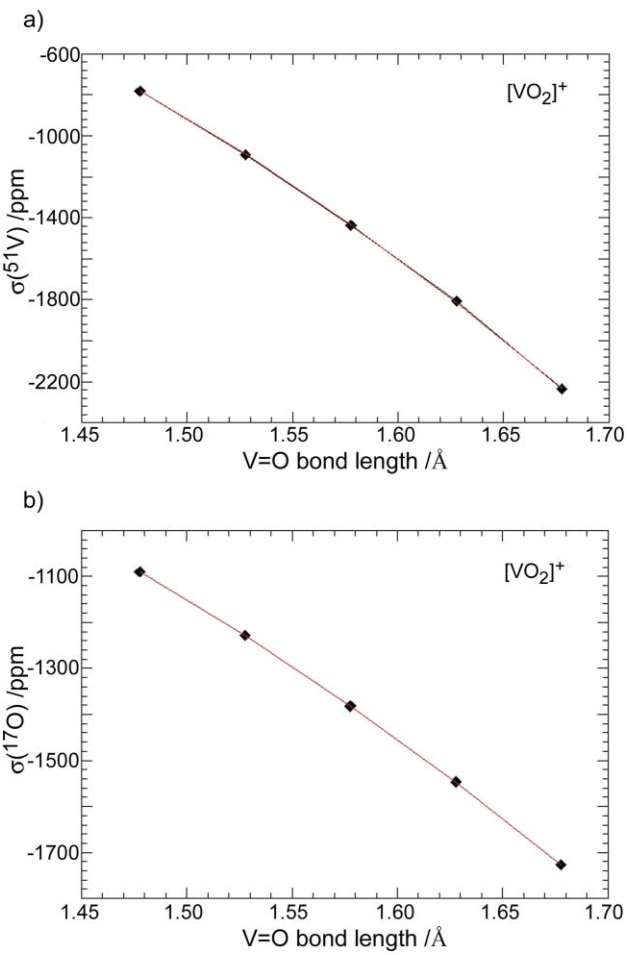

Fig. 5 Quadratic fits to the plots of the change in the magnetic shielding constants of (a) ^{51}V ($y = -8458.9 + 16151x - 7414.6x^2$) and (b) ^{17}O ($y = -3020.3 + 5260.5x - 2675.9x^2$) *vs.* V=O bond length for $[VO_2]^+$.

The plots of the ^{51}V and ^{17}O magnetic shielding constants adjust very well to quadratic fits, leading to the equations $y = -8458.9 + 16151x - 7414.6x^2$ for ^{51}V and $y = -3020.3 + 5260.5x - 2675.9x^2$ for ^{17}O. Interestingly, the corresponding parameters in these two equations are related by the factors 2.8, 3.1 and 2.8, respectively for a, b and c ($y = a + bx + cx^2$), which are very close to the ratio between the nuclear charges of the two nuclei, that is, $Z(V)/Z(O) = 2.9$. In the literature we found several reports of a correlation between ^{95}Mo and ^{183}W chemical shifts of homologous complexes.[27-29] For these, the correlation parameter is the ratio between the nuclear charges (one of the correlations is[29] $\delta_W = 1.8\delta_{Mo} - 137.3$). In our case, the different geometries of $[VO_2]^+$ as we change the V=O bond lengths can be seen as "homologous" complexes. However, we are analyzing a correlation between two atoms (V and O) that belong to the same molecule, that is, vanadium and oxygen are not in homologous chemical environments, so that our correlation is different from that described for W and Mo. If we further relate σ^{51}V as a function of σ^{17}O for $[VO_2]^+$ (with different V=O bond lengths) we get the linear relationship $\sigma^{51}V = 2.28\sigma^{17}O + 1706.4$, with a correlation coefficient of 0.99992 (Fig. 6). This means that the electronic structures around the V and O nuclei vary in a correlated manner.

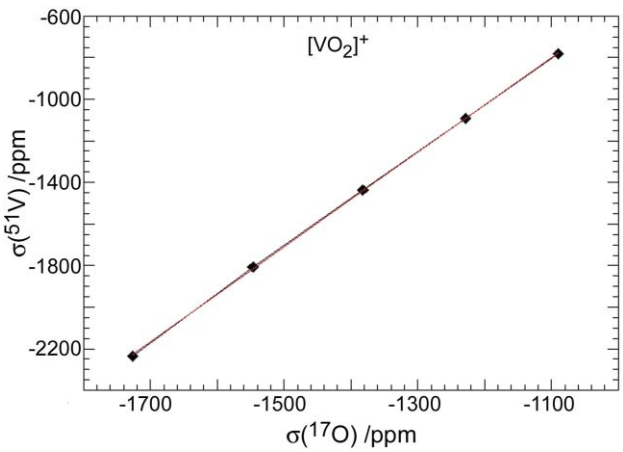

Fig. 6 Linear fit to the plot of σ^{51}V *vs.* σ^{17}O for the several VO_2^+ geometries considered in Fig. 5 (different V=O bond lengths); $y = 1706.4 + 2.28x$, correlation coefficient of 0.99992.

In addition to varying the V=O bond length, we have also studied the effect of varying the O=V=O angle. However, this parameter has, by comparison, a very small influence. The results are summarized in Table 7. It can be concluded that the length of the V=O bond is the dominant factor involved in the variation of the chemical shifts. We obtain gradients of $\Delta(\delta^{51}V)/\Delta(r V{=}O) \approx 6550$ ppm Å^{-1} and $\Delta(\delta^{17}O)/\Delta(r V{=}O) \approx 2920$ ppm Å^{-1}. The gradient of 6552 ppm Å^{-1} is due to the modification of two V=O bonds, thus, giving a gradient of *ca.* 3276 ppm Å^{-1} per bond. The O–V–O angle has an effect of the order of a few ppm per degree.

(b) Molecular model $[VO(OO)]^+$

The optimized structure of $[VO(OO)]^+$ is presented in Fig. 7. We have modified the bond lengths of V–O (one of the bonds), V=O, O–O, and the O=V–O angle. Figs. 8 and 9 show the plots for the V=O and V–O bond lengths, respectively. The results are summarized in Table 8.

Table 7 Effects on ^{51}V and ^{17}O chemical shifts of changes on the structure of $[VO_2]^+$ (UDFT-IGLO-PW91)

Structural parameter	$\Delta(\delta^{51}V)/\Delta$(parameter)	$\Delta(\delta^{17}O)/\Delta$(parameter)
r(V=O)[a] 1.4777 Å → 1.5777 Å	6552 ppm Å^{-1}	2921 ppm Å^{-1}
r(V=O)[a] 1.5777 Å → 1.6777 Å	7988 ppm Å^{-1}	3445 ppm Å^{-1}
∠(O–V–O) 100.15° → 106.15°	1.17 ppm degree^{-1}	–8.00 ppm degree^{-1}
∠(O–V–O) 106.15° → 112.15°	2.15 ppm degree^{-1}	–6.70 ppm degree^{-1}

[a] The lengths of both V=O bonds have been modified.

Table 8 Effects on ^{51}V and ^{17}O (V=O oxygen) chemical shifts of changes on the structure of $[VO(OO)]^+$ (UDFT-IGLO-PW91)

Structural parameter	$\Delta(\delta^{51}V)/\Delta$(parameter)	$\Delta(\delta^{17}O)/\Delta$(parameter)
r(V=O) 1.4668 Å → 1.6668 Å	3323 ppm Å^{-1}	2312 ppm Å^{-1}
r(V–OO)[a] 1.7349 Å → 1.9349 Å	2840 ppm Å^{-1}	315.1 ppm Å^{-1}
r(O–O) 1.3991 Å → 1.5991 Å	–752.5 ppm Å^{-1}	123.0 ppm Å^{-1}
∠(O–V=O) 103.45° → 109.45°	11.1 ppm degree^{-1}	–1.33 ppm degree^{-1}

[a] Only one V–OO has been modified.

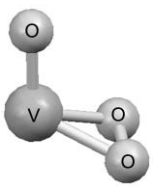

Fig. 7 SBKJC/B3LYP structure of $[VO(OO)]^+$.

In this case, due to the loss of symmetry compared with $[VO_2]^+$, the variation of electronic structure around the metal and the oxo oxygen atom are less dependent upon each other as we change the geometry, so that the correlations found for $[VO_2]^+$ do not hold. The correlation between the ^{51}V and ^{17}O chemical shifts is not linear in this case, but instead is quadratic ($\sigma^{51}V = 89.9 + 2.37\sigma^{17}O + 0.00042(\sigma^{17}O)^2$).

For this molecular model, similar to that observed for $[VO_2]^+$, the modification of the V=O bond length is the dominant factor in relation to the change in the metal and in the oxo oxygen chemical shifts due to geometry modifications. The gradient $\Delta(\delta^{51}V)/\Delta(r$V=O) is 3323 ppm Å^{-1}, a value which is extremely close to that obtained for $[VO_2]^+$ (3276 ppm Å^{-1} per bond) and is also close to the gradient obtained for **G-3** (2430 ppm Å^{-1}, Table 6). The gradient $\Delta(\delta^{17}O)/\Delta(r$V=O) is 2312 ppm Å^{-1}. The length of the V–OO bond is important only in the case of the ^{51}V chemical shift, with $\Delta(\delta^{51}V)/\Delta(r$V–OO) equal to 2840 ppm Å^{-1}, while the O–O bond length and the O–V=O angle have a significantly smaller weight in the determination of both chemical shifts. If, as a first approximation, we assume that these results can be transferred to the oxoperoxo complexes studied in this paper, these values indicate that, with the V=O bond, for example, an error of 0.02 Å (*ca.* 1.2% for a typical rV=O of 1.600 Å) in the calculation of the bond length implies an error of 66.5 ppm in the calculation of the ^{51}V chemical shift and an error of 46.2 ppm in the calculation of the ^{17}O chemical shift of the oxo oxygen.

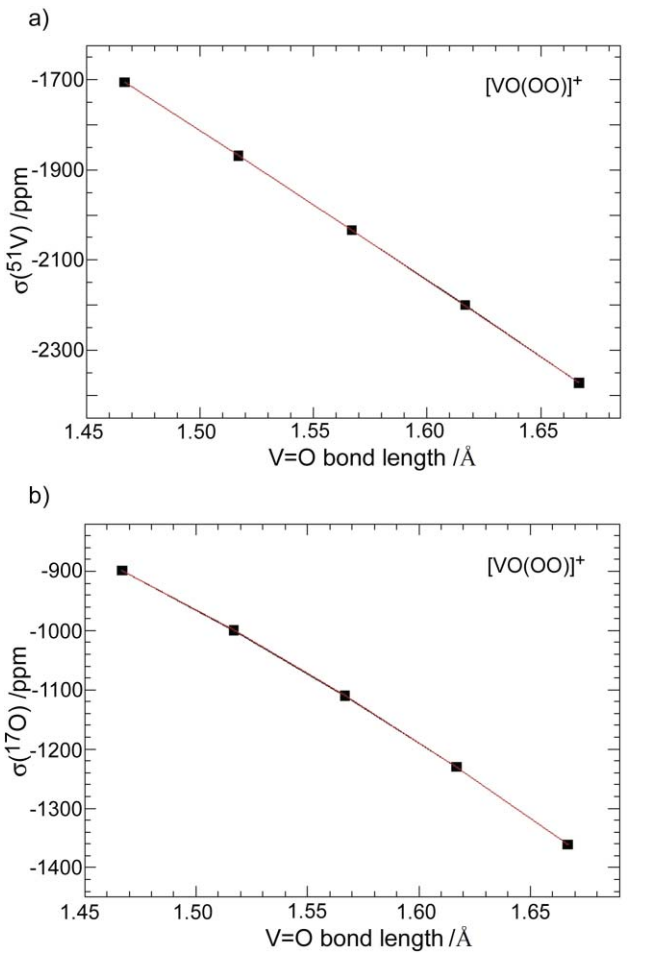

Fig. 8 Quadratic fits to the plots of the change in the magnetic shielding constants of (a) ^{51}V ($y = 1160.8 - 1395.7x - 613.78x^2$) and (b) ^{17}O of the V=O oxygen ($y = -2364.6 + 3911.8x - 1985.5x^2$) *vs.* V=O bond length for $[VO(OO)]^+$.

(c) Molecular model $[VO_2(gly)(H_2O)]^-$

In order to evaluate the possibility of transferring the conclusions above to coordinatively more saturated complexes, we have analyzed the same kind of effects on the system $[VO_2(gly)(H_2O)]^-$. Fig. 10 shows the optimized structure of this

Table 9 Effects on ^{51}V and ^{17}O (V=O oxygen) chemical shifts of changes on the structure of $[VO_2(gly)(H_2O)]^-$ (UDFT-IGLO-PW91)

Structural parameter	$\Delta(\delta^{51}V)/\Delta$(parameter)	$\Delta(\delta^{17}O)/\Delta$(parameter)
r(V=O)[a] 1.62324 Å → 1.66324 Å	4072.5 ppm Å^{-1}	1635.1 ppm Å^{-1}
r(V–OCH_2) 1.863162 Å → 1.903162 Å	942.5 ppm Å^{-1}	287.5 ppm Å^{-1}
r(V–OCO) 2.041383 Å → 2.081383 Å	305.0 ppm Å^{-1}	250.0 ppm Å^{-1}
r(VO–CO) 1.254635 Å → 1.454635 Å	−158.4 ppm Å^{-1}	−93.35 ppm Å^{-1}

[a] The lengths of both V=O bonds have been modified.

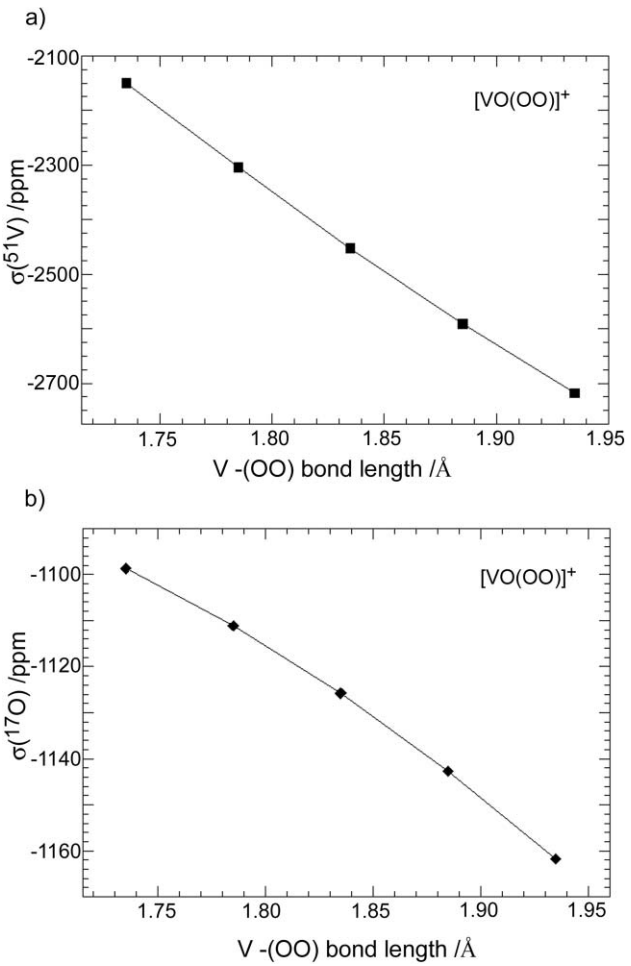

Fig. 9 Plots of the change in the magnetic shielding constants of (a) ^{51}V and (b) ^{17}O of the V=O oxygen *vs.* V–OO bond length for $[VO(OO)]^+$ (only one V–OO bond has been modified).

V(V) dioxo complex and Table 9 summarizes the $\Delta\delta/\Delta$(parameter) results.

Again, the V=O bond length is the major contribution in determining the ^{51}V and the oxo ^{17}O chemical shifts, with $\Delta(\delta^{51}V)/\Delta(r\text{V=O}) \approx 2036$ ppm Å^{-1} and $\Delta(\delta^{17}O)/\Delta(r\text{V=O}) \approx 818$ ppm Å^{-1} (per V=O bond). These values, however, are smaller than those obtained for $[VO_2]^+$ ($\Delta(\delta^{51}V)/\Delta(r\text{V=O}) \approx 3326$ ppm Å^{-1} and $\Delta(\delta^{17}O)/\Delta(r\text{V=O}) \approx 1460$ ppm Å^{-1}, per bond). As expected, the ^{51}V and ^{17}O chemical shifts suffer a smaller influence from the modification of bonds that are farther from the metal, as we can see for the VO–CO bond. In the literature, some

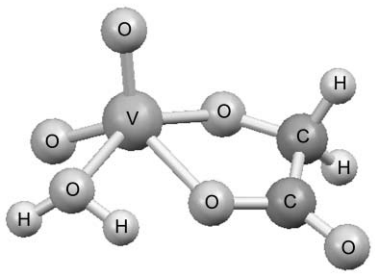

Fig. 10 SBKJC/B3LYP structure of $[VO_2(gly)(H_2O)]^-$.

$\partial\sigma/\partial r$ derivatives have been reported for related systems. For example, for the oxovanadium complexes $[VO(OCH_2CH_2)_3N]$, $[VO(CH_3)_3]$, $[VOCl_3]$, $[VOF_3]$, $[VOCl_2F]$, $[VO(CH_2Si(CH_3)_3)_3]$ and $[VO(CH_3)_3AlH_3]$, the values $\partial(\sigma^{51}V)/\partial(r\text{V=O})$ obtained were, respectively, −3270, −4330, −3220, −3400, −3720, −4250 and −3970 ppm Å^{-1}.[30] For the diperoxo complex $[VO(O_2)_2(Im)]^-$ (Im = imidazol) $\partial(\sigma^{51}V)/\partial(r\text{V–N}) = -719$ ppm Å^{-1} was obtained.[31] Note that the gradients we report from our study are presented as $\Delta\delta/\Delta r$ and the derivatives from references 30 and 31 are presented as $\partial\sigma/\partial r$.

Computational details

The molecular structures were optimized at DFT level without symmetry constraints using the GAMESS code.[32] The calculations employed the B3LYP hybrid functional (Becke three-parameter Lee–Yang–Parr)[33,34] and the relativistic SBKJC[35,36] effective core potentials (ECPs) and valence basis sets. The gradient threshhold for optimizations was taken as 10^{-5} hartree bohr^{-1}. The energy Hessian was calculated for the resultant stationary points, and all were characterized as true minima (*i.e.*, no imaginary frequencies).

Based on the optimized structures, nuclear shieldings have been computed at DFT level[37-41] with individual gauges for localized orbitals (IGLO).[42] These calculations used the deMon program[43,44] (including the deMon-NMR modules[45,46]) and the PW91[47-49] gradient-corrected functional. The calculations employed a 9s7p4d all-electron basis for V,[50-52] the IGLO-II[42] all electron basis sets for O, C and H, and a fine integration grid (FINE option). In addition to the standard uncoupled DFT (UDFT) equations arising from the use of a GGA functional,[37-41] we have also evaluated the use of the "Malkin correction" in its LOC1 approximation within the sum-over-states density-functional perturbation theory (SOS-DFPT) approach.[45,46] However, the effect on the most important ^{51}V and ^{17}O shifts was minor, and we will thus report only the UDFT results. ^{13}C and ^{1}H relative chemical shifts (δ) are given with respect to the absolute shielding values (σ)

of tetramethylsilane (TMS) obtained at the same computational level, and ^{51}V shifts are given with respect to the shielding value of $VOCl_3$. Calculated ^{17}O nuclear shieldings have been converted to chemical shifts using a shielding value of +290.9 ppm for liquid water at room temperature, derived from the absolute shielding scale of ref. 53.

Conclusions

In view of the relevance of vanadium compounds for both biological and industrial applications, we have carried out a DFT study of the structures and structural correlations with NMR chemical shifts of oxoperoxo and dioxo V(V) complexes. The DFT predicted structures were tested by comparing their theoretical NMR chemical shifts with the experimental solution values. The computational methodologies used allowed us to obtain theoretical chemical shifts which are, in most cases, in good agreement with the experimental values, thus suggesting the correctness of the proposed structures.

From the analysis of the effects of structural changes on the metal magnetic shielding, we concluded that in peroxo V(V) species this property is mainly dependent on the geometry involving the metal nucleus and the replacement of substituents far from the metal does not significantly affect its magnetic shielding. This finding explains why it is possible to establish reference scales that correlate the type of complex with its typical region of ^{51}V chemical shifts. These studies were extended to small molecules used in quantitative analysis. This also allows the important conclusion that the ^{51}V and ^{17}O chemical shifts are extremely sensitive to the V=O bond lengths in the oxoperoxo and in the dioxo centres. For the three model systems analyzed, the V=O bond length is the major factor determining $\delta^{51}V$.

$\Delta\delta/\Delta$(geometrical parameter) values were obtained for the models $[VO_2]^+$ and $[VO(OO)]^+$. These, to a first approximation, can also be transferred to larger complexes. In cases where the effects of the substituents are not substantial, this may allow the prediction of changes in the ^{51}V and ^{17}O chemical shifts between complexes based on their structural differences.

Acknowledgements

L.L.G.J. wishes to thank "Fundação para a Ciência e a Tecnologia", of the Portuguese Ministry for Science, Technology and Higher Education, for the postdoctoral grant SFRH/BPD/26415/2006 and the "Laboratório de Computação Avançada", of the Department of Physics of the University of Coimbra, for the computing facilities (Milipeia Cluster).

References

1 D. Rehder, *Angew. Chem., Int. Ed. Engl.*, 1991, **30**, 148–167 and references therein.
2 P. J. Stankiewicz and A. S. Tracey, in Vanadium and its Role in Life in *Metal Ions in Biological Systems*, ed. H. Sigel and A. Sigel, Marcel Dekker, New York, 1995, vol. 31, pp. 265–266.
3 C. Djordjevic, *Met. Ions Biol. Syst.*, 1995, **31**, 595–616.
4 A. M. Evangelou, *Crit. Rev. Oncol. Hematol.*, 2002, **42**, 249–265.
5 H. Sakurai, Y. Kojima, Y. Yoshikawa, K. Kawabe and H. Yasui, *Coord. Chem. Rev.*, 2002, **226**, 187–198.
6 K. H. Thompson, J. H. McNeill and C. Orvig, *Chem. Rev.*, 1999, **99**, 2561–2572.
7 D. C. Crans, J. J. Smee, E. Gaidamauskas and L. Yang, *Chem. Rev.*, 2004, **104**, 849–902 and references therein.
8 G. J. Colpas, B. J. Hamstra, J. W. Kampf and V. L. Pecoraro, *J. Am. Chem. Soc.*, 1994, **116**, 3627–3628.
9 G. J. Colpas, B. J. Hamstra, J. W. Kampf and V. L. Pecoraro, *J. Am. Chem. Soc.*, 1996, **118**, 3469–3478.
10 K. Kanamori, K. Nishida, N. Miyata and K. Okamoto, *Chem. Lett.*, 1998, 1267–1268.
11 T. Hirao, *Chem. Rev.*, 1997, **97**, 2707–2724.
12 C. Bolm, *Coord. Chem. Rev.*, 2003, **237**, 245–256.
13 E. Tsuchida and K. Oyaizu, *Coord. Chem. Rev.*, 2003, **237**, 213–228.
14 L. L. G. Justino, M. L. Ramos, M. M. Caldeira and V. M. S. Gil, *Eur. J. Inorg. Chem.*, 2000, 1617–1621.
15 L. L. G. Justino, M. L. Ramos, M. M. Caldeira and V. M. S. Gil, *Inorg. Chim. Acta*, 2000, **311**, 119–125.
16 L. L. G. Justino, M. L. Ramos, M. M. Caldeira and V. M. S. Gil, *Inorg. Chim. Acta*, 2003, **356**, 179–186.
17 L. L. G. Justino, M. L. Ramos, F. Nogueira, A. J. F. N. Sobral, C. F. G. C. Geraldes, M. Kaupp, H. D. Burrows, C. Fiolhais and V. M. S. Gil, *Inorg. Chem.*, 2008, **47**, 7317–7326.
18 P. Švančárek, P. Schwendt, J. Tatiersky, I. Smatanová and J. Marek, *Monatsh. Chem.*, 2000, **131**, 145–154.
19 P. Schwendt, P. Švančárek, I. Smatanová and J. Marek, *J. Inorg. Biochem.*, 2000, **80**, 59–64.
20 M. Bühl and M. Parrinello, *Chem.–Eur. J.*, 2001, **7**, 4487–4494 and references therein.
21 M. Bühl, *J. Comput. Chem.*, 1999, **20**, 1254–1261.
22 M. Bühl and F. Hamprecht, *J. Comput. Chem.*, 1998, **19**, 113–122.
23 M. S. Reynolds and A. Butler, *Inorg. Chem.*, 1996, **35**, 2378–2383.
24 V. Conte, F. Di Furia and S. Moro, *J. Mol. Catal. A: Chem.*, 1995, **104**, 159–169.
25 D. Rehder, in *Vanadium in Biological Systems*, ed. N. D. Chasteen, Kluwer Academic Publishers, Dordrecht, 1990, ch. X, p. 173.
26 D. Rehder, C. Weidemmann, A. Duch and W. Priebsch, *Inorg. Chem.*, 1988, **27**, 584–587.
27 M. Minelli, J. Enemark, R. T. C. Brownlee, M. J. O'Connor and A. G. Wedd, *Coord. Chem. Rev.*, 1985, **68**, 169–278.
28 Y. Ma, P. Demou and J. W. Faller, *Inorg. Chem.*, 1991, **30**, 62–64.
29 M. L. Ramos, M. M. Caldeira and V. M. S. Gil, *J. Chem. Soc., Dalton Trans.*, 2000, 2099–2103.
30 S. Grigoleit and M. Bühl, *Chem.–Eur. J.*, 2004, **10**, 5541–5552.
31 M. Bühl, R. Schurhammer and P. Imhof, *J. Am. Chem. Soc.*, 2004, **126**, 3310–3320.
32 M. W. Schmidt, K. K. Baldridge, J. A. Boatz, S. T. Elbert, M. S. Gordon, J. H. Jensen, S. Koseki, N. Matsunaga, K. A. Nguyen, S. J. Su, T. L. Windus, M. Dupuis and J. A. Montgomery, *J. Comput. Chem.*, 1993, **14**, 1347–1363.
33 A. D. Becke, *J. Chem. Phys.*, 1993, **98**, 5648–5652.
34 C. Lee, W. Yang and R. G. Parr, *Phys. Rev. B: Condens. Matter Mater. Phys.*, 1988, **37**, 785–789.
35 W. J. Stevens, M. Krauss, H. Basch and P. G. Jasien, *Can. J. Chem.*, 1992, **70**, 612–630.
36 T. R. Cundari and W. J. Stevens, *J. Chem. Phys.*, 1993, **98**, 5555–5565.
37 V. G. Malkin, O. L. Malkina and D. R. Salahub, *Chem. Phys. Lett.*, 1993, **204**, 80–86.
38 V. G. Malkin, O. L. Malkina and D. R. Salahub, *Chem. Phys. Lett.*, 1993, **204**, 87–95.
39 G. Schreckenbach and T. Ziegler, *J. Phys. Chem.*, 1995, **99**, 606–611.
40 G. Rauhut, S. Puyear, K. Wolinski and P Pulay, *J. Phys. Chem.*, 1996, **100**, 6310–6316.
41 J. R. Cheeseman, G. W. Trucks, T. A. Keith and M. Frisch, *J. Chem. Phys.*, 1996, **104**, 5497–5509.
42 W. Kutzelnigg, U. Fleischer and M. Schindler, in *NMR-Basic Principles and Progress*, Springer, Heidelberg, 1990, vol. 23, p. 167.
43 D. R Salahub, R. Fournier, P. Mlynarski, I. Papai, A. St-Amant and J. Ushio, in *Density Functional Methods in Chemistry*, ed. J. Labanowski and J. Andzelman, Springer, New York, 1991.
44 A. St-Amant and D. R Salahub, *Chem. Phys. Lett.*, 1990, **169**, 387–392.
45 V. G. Malkin, O. L. Malkina, M. E. Casida and D. R. Salahub, *J. Am. Chem. Soc.*, 1994, **116**, 5898–5908.
46 V. G. Malkin, O. L. Malkina, L. A. Eriksson and D. R. Salahub, in *Modern Density Functional Theory: A Tool for Chemistry; Theoretical and Computational Chemistry*, ed. J. M. Seminario and P. Politzer, Elsevier, Amsterdam, 1995, vol. 2.

47 J. P. Perdew and Y. Wang, *Phys. Rev. B: Condens. Matter Mater. Phys.*, 1992, **45**, 13244–13249.
48 J. P. Perdew, in *Electronic Structure of Solids*, ed. P. Ziesche and H. Eischrig, Akademie Verlag, Berlin, 1991.
49 J. P. Perdew, J. A. Chevary, S. H. Vosko, K. A. Jackson, M. R. Pederson, D. J. Singh and C. Fiolhais, *Phys. Rev. B: Condens. Matter Mater. Phys.*, 1992, **46**, 6671–6687.
50 M. Dolg, U. Wedig, H. Stoll and H. Preuss, *J. Chem. Phys.*, 1987, **86**, 866–872.
51 A. Schäfer, H. Horn and R. Ahlrichs, *J. Chem. Phys.*, 1992, **97**, 2571–2577.
52 M. Munzarová and M. Kaupp, *J. Phys. Chem. A*, 1999, **103**, 9966–9983.
53 D. Sundholm, J. Gauss and A. Schäfer, *J. Chem. Phys.*, 1996, **105**, 11051–11059.